

# Measurement of high-frequency rotational transitions of $\text{H}_2\text{O}^+$ in its ground state by far-infrared laser magnetic resonance (LMR) spectroscopy

P. Mürzt,<sup>a)</sup> L. R. Zink, and K. M. Evenson

*Time and Frequency Division, National Institute of Standards and Technology (NIST), 325 Broadway, Boulder, Colorado 80303*

J. M. Brown

*Physical and Theoretical Chemistry Laboratory, South Parks Road, Oxford OX1 3QZ, United Kingdom*

(Received 18 August 1998; accepted 31 August 1998)

Thirteen new rotational transitions of  $\text{H}_2\text{O}^+$  in the (0,0,0) level of the  $\tilde{X}^2B_1$  state have been measured in the wavenumber region between 80 and 200  $\text{cm}^{-1}$  (50 and 120  $\mu\text{m}$ ) by far-infrared laser magnetic resonance (LMR) spectroscopy. LMR data measured previously between 25 and 90  $\text{cm}^{-1}$  (110 and 400  $\mu\text{m}$ ), as well as optical and infrared combination differences, have been combined with the new LMR data in a weighted least-squares analysis using an A-reduced expression of the rotational-fine structure Hamiltonian. Thirty-two molecular constants were simultaneously determined, some sextic centrifugal distortion parameters and some quartic and sextic spin-rotation parameters for the first time. From this improved set of molecular parameters, very accurate calculations of rotational term values and zero-field predictions of the  $1_{11}-0_{00}$  transition, including hyperfine structure, have been performed. Moreover, the electronic  $g$ -tensors and the hyperfine coupling constants are consistent with *ab initio* calculations which had been carried out for these constants. © 1998 American Institute of Physics. [S0021-9606(98)00746-6]

## I. INTRODUCTION

The water cation ( $\text{H}_2\text{O}^+$ ) has been of interest to spectroscopists and astrophysicists since the early 1950's, when it was postulated to be present in comet tails. The first high-resolution spectroscopy of  $\text{H}_2\text{O}^+$  was done by Lew and Heiber,<sup>1,2</sup> when they investigated the  $\tilde{A}^2A_1-\tilde{X}^2B_1$  electronic emission spectrum. It resulted in the identification of visible emission lines from  $\text{H}_2\text{O}^+$  in Comet Kohoutek<sup>3,4</sup> and subsequently in other comets. Moreover,  $\text{H}_2\text{O}^+$  plays an important role in elementary processes in interstellar space<sup>5</sup> and in the earth's upper atmosphere.<sup>6</sup>

Several other high-resolution absorption measurements have been performed on  $\text{H}_2\text{O}^+$ . The visible system of  $\text{H}_2\text{O}^+$  has been observed using laser absorption spectroscopy.<sup>7</sup> Some pure rotational transitions have been measured by far-infrared laser magnetic resonance spectroscopy (LMR),<sup>8</sup> which permitted the observation of the proton hyperfine structure. A few lines of the rotational spectrum around 430  $\text{cm}^{-1}$ , measured by diode lasers, are reported in, Ref. 9, but those lines could not be assigned up to now. In the IR region, the  $\nu_3$  band has been characterized using a difference frequency spectrometer,<sup>10</sup> the  $\nu_2$  and the  $2\nu_2-\nu_2$  bands using a diode laser spectrometer,<sup>11</sup> and the  $\nu_1$  and the  $\nu_2+\nu_3-\nu_2$  bands by color-center laser spectroscopy.<sup>12</sup> Recently, new vibronic bands in the near-infrared region were observed.<sup>13</sup>

A number of *ab initio* calculations have been carried out for  $\text{H}_2\text{O}^+$ , see, for example, Ref. 14 and references therein. Some of them investigated the hyperfine coupling constants of the ground state.<sup>14,15</sup> Recently, a multireference configu-

ration interaction calculation of electronic  $g$ -tensors has been carried out.<sup>16</sup>

In this work, we measure 13 new rotational transitions of  $\text{H}_2\text{O}^+$  in its ground state, which prompts a reinvestigation of

TABLE I. Summary of the FIR laser lines used and the  $\text{H}_2\text{O}^+$  transitions observed.

Calculated wavelength [ $\mu\text{m}$ ]		Laser line		H <sub>2</sub> O <sup>+</sup> transition
Measured frequency [MHz]	Gas	Pump line CO <sub>2</sub> laser	Assignment	
115.823	<sup>13</sup> CH <sub>3</sub> OH	10R(16)	5 <sub>24</sub> -5 <sub>15</sub>	
100.806	CH <sub>3</sub> OH	9R(14)	2 <sub>20</sub> -1 <sub>11</sub> 6 <sub>25</sub> -6 <sub>16</sub> 5 <sub>15</sub> -3 <sub>22</sub>	
88.948	<sup>13</sup> CH <sub>3</sub> OH	9P(44)	7 <sub>26</sub> -7 <sub>17</sub> 3 <sub>22</sub> -2 <sub>11</sub> 4 <sub>04</sub> -2 <sub>11</sub>	
81.917	CH <sub>3</sub> OH	9P(26)	4 <sub>40</sub> -4 <sub>31</sub> 5 <sub>42</sub> -5 <sub>33</sub>	
81.557	CD <sub>3</sub> OH	10R(16)	4 <sub>40</sub> -4 <sub>31</sub> 5 <sub>42</sub> -5 <sub>33</sub>	
77.905	CH <sub>3</sub> OH	10R(16)	3 <sub>21</sub> -2 <sub>12</sub> 4 <sub>23</sub> -3 <sub>12</sub>	
63.096	<sup>13</sup> CH <sub>3</sub> OH	9P(12)	4 <sub>22</sub> -3 <sub>13</sub>	
62.966	CH <sub>3</sub> OH	10R(16)	4 <sub>22</sub> -3 <sub>13</sub>	
56.728	CH <sub>3</sub> OH	9R(16)	4 <sub>31</sub> -3 <sub>22</sub>	

<sup>a)</sup>Taken from Ref. 23 (there is a misprint in Ref. 24).

<sup>b)</sup>Taken from Ref. 24.

<sup>c)</sup>Remeasured during this work (the measurement of 3363537.3 MHz in Ref. 19 is incorrect, see text).

<sup>d)</sup>Measured during this work (it had not been measured previously).

<sup>a)</sup>Present address: Radiologische Klinik, Universität Bonn, Sigmund-Freud-Str. 25, D-53105 Bonn, Germany. Electronic mail: muertz@imsdd.meb.uni-bonn.de

TABLE II. Zeeman resonances observed and calculations of tuning rates and transition frequencies for zero field.

$N'$	$K'$	$P'$	$2J'$	$2M'_j$	$2M'_l$	$N''$	$K''$	$P''$	$2J''$	$2M''_j$	$2M''_l$	$B_{obs}$ [ $10^{-4}$ T]	$\Delta\nu^a$ [ $10^{-5}$ cm $^{-1}$ ]	$\Delta\nu_{obs}^b$ [ $10^{-5}$ cm $^{-1}$ ]	$TR^c$ [ $10^4$ MHz/T]	$\nu_{cal}(B=0)^d$ [cm $^{-1}$ ]
$\nu_L = 86.338453$ cm $^{-1}$ (115.823 $\mu$ m, $^{13}$ CH $_3$ OH, CO $_2$ pump: 10R(16))																
5	2	1	11	9	-2	5	1	-1	11	9	-2	5738.8	0.03	4.2	1.80	86.15910
5	2	1	11	9	0	5	1	-1	11	9	0	5768.7	-0.43	4.2	1.80	86.15919
5	2	1	11	9	2	5	1	-1	11	9	2	5798.5	0.60	4.2	1.80	86.15930
5	2	1	11	7	-2	5	1	-1	11	7	-2	6270.3	-1.14	3.2	1.31	86.15910
5	2	1	11	7	0	5	1	-1	11	7	0	6298.4	-0.83	3.2	1.31	86.15919
5	2	1	11	7	2	5	1	-1	11	7	2	6326.6	-0.39	3.2	1.31	86.15930
5	2	1	11	5	-2	5	1	-1	11	5	-2	7105.6	-1.10	2.9	0.95	86.15910
5	2	1	11	5	0	5	1	-1	11	5	0	7131.8	0.07	2.9	0.95	86.15919
5	2	1	11	5	2	5	1	-1	11	5	2	7158.6	-0.33	2.9	0.95	86.15930
5	2	1	9	9	-2	5	1	-1	9	9	-2	16765.2	-1.16	2.8	-0.33	86.89147
5	2	1	9	9	0	5	1	-1	9	9	0	16804.8	0.66	2.8	-0.33	86.89135
5	2	1	9	9	2	5	1	-1	9	9	2	16845.1	3.16	2.8	-0.33	86.89120
$\nu_L = 99.199981$ cm $^{-1}$ (100.806 $\mu$ m, CH $_3$ OH, CO $_2$ pump: 9R(14))																
2	2	1	5	-1	-2	1	1	-1	3	-3	-2	2776.5	-2.76	2.6	0.94	99.10609
2	2	1	5	-1	0	1	1	-1	3	-3	0	2801.0	-0.56	2.6	0.94	99.10503
2	2	1	5	-1	2	1	1	-1	3	-3	2	2826.1	0.48	2.6	0.94	99.10355
2	2	1	5	1	-2	1	1	-1	3	-1	-2	3402.6	-0.99	2.6	0.90	99.10412
2	2	1	5	1	0	1	1	-1	3	-1	0	3426.8	0.26	2.6	0.90	99.10306
2	2	1	5	1	2	1	1	-1	3	-1	2	3451.9	-0.65	2.6	0.90	99.10355
2	2	1	5	3	-2	1	1	-1	3	1	-2	4574.3	-0.71	2.6	0.88	99.10293
2	2	1	5	3	0	1	1	-1	3	1	0	4596.3	2.87	2.6	0.87	99.10306
2	2	1	5	3	2	1	1	-1	3	1	2	4619.8	2.42	2.6	0.87	99.10355
6	2	-1	11	7	0	6	1	1	11	5	0	3591.5	0.07	2.7	-1.12	99.28624
6	2	-1	11	5	0	6	1	1	11	3	0	3806.2	-0.24	2.5	-0.97	99.28624
6	2	-1	11	3	0	6	1	1	11	1	0	4112.5	-0.38	2.4	-0.82	99.28624
6	2	-1	11	7	0	6	1	1	11	7	0	4288.3	-0.35	2.8	-1.10	99.28624
6	2	-1	11	5	0	6	1	1	11	7	0	5466.4	1.03	2.7	-0.89	99.28624
6	2	-1	11	3	0	6	1	1	11	5	0	5976.4	-0.89	2.5	-0.70	99.28624
6	2	-1	11	-3	0	6	1	1	11	-5	0	6108.9	-0.99	4.5	-0.40	99.28624
5	1	-1	11	7	-2	3	2	1	7	5	-2	13260.9	9.10	6.0	-1.03	99.75148
5	1	-1	11	7	0	3	2	1	7	5	0	13285.9	3.84	6.0	-1.03	99.75118
5	1	-1	11	7	2	3	2	1	7	5	2	13311.1	-0.93	6.0	-1.03	99.75096
$\nu_L = 112.424607$ cm $^{-1}$ (88.948 $\mu$ m, $^{13}$ CH $_3$ OH, CO $_2$ pump: 9P(44))																
7	2	1	15	13	-2	7	1	-1	13	11	-2	2592.8	-0.74	3.0	1.06	112.27321
7	2	1	15	13	0	7	1	-1	13	11	0	2633.6	0.38	3.0	1.06	112.27032
7	2	1	15	13	2	7	1	-1	13	11	2	2675.1	1.23	3.0	1.05	112.26704
3	2	1	5	1	-2	2	1	-1	3	3	-2	1955.4	2.20	2.3	0.48	112.38689
3	2	1	5	1	0	2	1	-1	3	3	0	1994.5	0.54	2.3	0.47	112.38685
3	2	1	5	1	2	2	1	-1	3	3	2	2033.3	0.56	2.3	0.47	112.38655
3	2	1	5	5	-2	2	1	-1	5	5	-2	8433.6	8.25	5.9	-1.95	113.03364
3	2	1	5	5	0	2	1	-1	5	5	0	8461.2	8.08	5.9	-1.95	113.03586
3	2	1	5	5	2	2	1	-1	5	5	2	8489.0	8.62	5.9	-1.95	113.03896
3	2	1	5	3	-2	2	1	-1	5	5	-2	13666.6	2.11	4.2	-0.76	113.03364
3	2	1	5	3	0	2	1	-1	5	5	0	13696.9	2.72	4.2	-0.76	113.03586
3	2	1	5	3	2	2	1	-1	5	5	2	13727.1	2.91	4.2	-0.76	113.03896
4	0	1	9	-3	-2	2	1	-1	3	-1	-2	2087.1	-2.14	3.7	-1.65	112.51721
4	0	1	9	-3	0	2	1	-1	3	-1	0	2113.6	-0.08	3.7	-1.65	112.51572
4	0	1	9	-3	2	2	1	-1	3	-1	2	2139.7	-2.05	3.7	-1.65	112.51238
4	0	1	9	-1	-2	2	1	-1	3	-1	-2	2389.2	1.50	3.0	-1.63	112.51721
4	0	1	9	-1	0	2	1	-1	3	-1	0	2414.2	1.50	3.0	-1.63	112.51572
4	0	1	9	-1	2	2	1	-1	3	-1	2	2439.3	0.73	3.0	-1.63	112.51238
4	0	1	9	1	-2	2	1	-1	3	1	-2	3841.2	-0.03	3.8	-1.44	112.51814
4	0	1	9	1	0	2	1	-1	3	1	0	3863.0	-0.57	3.8	-1.44	112.51572
4	0	1	9	1	2	2	1	-1	3	1	2	3885.2	0.71	3.8	-1.44	112.51238
4	0	1	9	1	-2	2	1	-1	3	3	-2	5265.2	-4.10	3.5	-1.13	112.51814
4	0	1	9	1	0	2	1	-1	3	3	0	5283.8	-1.36	3.5	-1.13	112.51572
4	0	1	9	1	2	2	1	-1	3	3	2	5302.3	1.02	3.5	-1.12	112.51238
4	0	1	9	3	-2	2	1	-1	3	3	-2	6357.0	0.86	3.8	-1.38	112.51814
4	0	1	9	3	0	2	1	-1	3	3	0	6378.0	-0.26	3.8	-1.38	112.51572
4	0	1	9	3	2	2	1	-1	3	3	2	6399.3	-0.29	3.8	-1.38	112.51238
4	0	1	9	5	-2	2	1	-1	3	3	-2	6796.5	-2.30	4.8	-1.75	112.51814
4	0	1	9	5	0	2	1	-1	3	3	0	6819.5	-2.49	4.8	-1.75	112.51572
4	0	1	9	5	2	2	1	-1	3	3	2	6842.7	-1.93	4.8	-1.75	112.51238
4	0	1	9	7	-2	2	1	-1	5	5	-2	10536.7	4.36	10.0	-2.62	113.16340
4	0	1	9	7	0	2	1	-1	5	5	0	10565.6	3.58	10.0	-2.62	113.16473
4	0	1	9	7	2	2	1	-1	5	5	2	10594.6	3.05	10.0	-2.62	113.16479
4	0	1	9	5	-2	2	1	-1	5	5	-2	10468.3	7.64	7.9	-2.07	113.16488
3	2	1	5	5	0	2	1	-1	5	5	0	10495.9	6.04	7.9	-2.07	113.03710
4	0	1	9	5	2	2	1	-1	5	5	2	10523.9	6.68	7.9	-2.07	113.16479

TABLE II. (Continued.)

$N'$	$K'$	$P'$	$2J'$	$2M'_j$	$2M'_l$	$N''$	$K''$	$P''$	$2J''$	$2M''_j$	$2M''_l$	$B_{obs}$ [ $10^{-4}$ T]	$\Delta\nu^a$ [ $10^{-5}$ cm $^{-1}$ ]	$\Delta\nu_{obs}^b$ [ $10^{-5}$ cm $^{-1}$ ]	$TR^c$ [ $10^4$ MHz/T]	$\nu_{cal}(B=0)^d$ [cm $^{-1}$ ]
$\nu_L = 122.074602$ cm $^{-1}$ (81.917 $\mu$ m, CH $_3$ OH, CO $_2$ pump: 9P(26))																
4	4	1	9	9	-2	4	3	-1	9	7	-2	19153.7	-7.72	13.1	1.46	121.58380
4	4	1	9	9	0	4	3	-1	9	7	0	19174.8	-10.15	13.1	1.46	121.58405
4	4	1	9	9	2	4	3	-1	9	7	2	19195.8	-12.00	13.1	1.46	121.58435
5	4	1	11	9	-2	5	3	-1	11	11	-2	15353.3	1.92	5.9	-0.65	122.28327
5	4	1	11	9	0	5	3	-1	11	11	0	15387.5	3.01	5.9	-0.65	122.28343
5	4	1	11	9	2	5	3	-1	11	11	2	15421.6	3.75	5.9	-0.65	122.28363
$\nu_L = 122.613488$ cm $^{-1}$ (81.557 $\mu$ m, CD $_3$ OH, CO $_2$ pump: 10R(16))																
4	4	1	7	5	2	4	3	-1	7	5	0	17761.0	8.95	62.0	-0.93	122.97353♣
4	4	1	7	5	0	4	3	-1	7	3	0	19485.0	45.94	47.1	-0.72	122.97353♣
5	4	1	11	11	-2	5	3	-1	11	9	-2	15670.3	4.28	10.6	1.24	122.28327
5	4	1	11	11	0	5	3	-1	11	9	0	15692.5	4.89	10.6	1.24	122.28343
5	4	1	11	11	2	5	3	-1	11	9	0	15715.4	2.72	10.6	1.24	122.28363
5	4	1	11	9	-2	5	3	-1	11	7	-2	16550.4	3.65	8.5	0.96	122.28327
5	4	1	11	9	0	5	3	-1	11	7	0	16573.1	0.74	8.5	0.96	122.28343
5	4	1	11	9	2	5	3	-1	11	7	2	16595.5	-1.13	8.5	0.96	122.28363
5	4	1	11	7	-2	5	3	-1	11	5	-2	17938.9	-2.08	7.1	0.76	122.28327
5	4	1	11	7	0	5	3	-1	11	5	0	17960.8	-3.98	7.1	0.76	122.28343
5	4	1	11	7	2	5	3	-1	11	5	2	17983.0	-6.57	7.1	0.76	122.28363
$\nu_L = 128.361651$ cm $^{-1}$ (77.905 $\mu$ m, CH $_3$ OH, CO $_2$ pump: 10R(16))																
3	2	-1	5	-3	0	2	1	1	5	-3	0	8498.3	-14.81	9.5	2.36	127.78729
3	2	-1	5	-1	0	2	1	1	5	-1	0	10762.9	-10.73	10.3	2.21	127.78729
3	2	-1	5	1	0	2	1	1	5	-1	0	12449.6	0.50	10.4	2.12	127.78729
3	2	-1	5	1	0	2	1	1	5	1	0	13771.5	-9.55	11.8	2.17	127.78729
3	2	-1	5	3	0	2	1	1	5	1	0	16082.1	-0.13	12.6	2.15	127.78729
3	2	-1	5	3	0	2	1	1	5	3	0	17609.9	-12.07	14.6	2.25	127.78729
4	2	-1	7	3	0	3	1	1	7	1	0	14255.9	-30.54	14.9	2.17	127.83222
4	2	-1	7	5	0	3	1	1	7	3	0	17303.3	-29.66	15.2	2.29	127.83222
$\nu_L = 158.487673$ cm $^{-1}$ (63.096 $\mu$ m, $^{13}$ CH $_3$ OH, CO $_2$ pump: 9P(12))																
4	2	1	9	5	-2	3	1	-1	7	3	-2	3207.9	-0.49	4.3	0.96	158.42612
4	2	1	9	5	0	3	1	-1	7	3	0	3233.2	-1.76	4.3	0.96	158.42619
4	2	1	9	5	2	3	1	-1	7	3	2	3258.8	-3.39	4.3	0.96	158.42637
4	2	1	9	7	-2	3	1	-1	7	5	-2	3564.1	-0.79	4.9	1.12	158.42612
4	2	1	9	7	0	3	1	-1	7	5	0	3590.6	-3.35	4.9	1.11	158.42619
4	2	1	9	7	2	3	1	-1	7	5	2	3616.6	-3.37	4.9	1.11	158.42637
4	2	1	9	5	0	3	1	-1	7	5	0	5102.4	0.55	7.9	1.05	158.42619
4	2	1	9	5	2	3	1	-1	7	5	2	5130.1	0.53	7.9	1.04	158.42637
4	2	1	9	-3	0	3	1	-1	7	-3	0	5642.9	-3.71	12.0	0.35	158.42619♣
4	2	1	9	-5	0	3	1	-1	7	-5	0	6966.5	-5.73	7.9	0.22	158.42619♣
$\nu_L = 158.815950$ cm $^{-1}$ (62.966 $\mu$ m, CH $_3$ OH, CO $_2$ pump: 10R(16))																
4	2	1	9	7	-2	3	1	-1	7	5	-2	10294.5	2.89	5.1	1.23	158.42612
4	2	1	9	7	0	3	1	-1	7	5	0	10324.6	3.12	5.1	1.23	158.42619
4	2	1	9	7	2	3	1	-1	7	5	2	10354.4	4.93	5.1	1.23	158.42637
4	2	1	7	7	-2	3	1	-1	5	5	-2	10709.8	-2.52	5.1	-1.16	159.21878
4	2	1	7	7	0	3	1	-1	5	5	0	10737.5	-4.46	5.1	-1.16	159.21872
4	2	1	7	7	2	3	1	-1	5	5	2	10765.8	-4.38	5.1	-1.16	159.21851
4	2	1	7	7	-2	3	1	-1	7	7	-2	13120.4	-1.42	5.1	-0.87	159.61856
4	2	1	7	7	0	3	1	-1	7	7	0	13156.9	-1.42	5.1	-0.87	159.62110
4	2	1	7	7	2	3	1	-1	7	7	2	13193.7	-0.81	5.1	-0.87	159.62436
$\nu_L = 176.279007$ cm $^{-1}$ (56.728 $\mu$ m, CH $_3$ OH, CO $_2$ pump: 9R(16))																
4	3	-1	7	-3	0	3	2	1	5	-5	0	9485.4	-1.79	13.5	-0.38	176.42473♣
4	3	-1	7	-1	0	3	2	1	5	-3	0	9626.8	1.73	13.5	-0.42	176.42597♣
4	3	-1	7	1	0	3	2	1	5	-1	0	9788.7	-0.25	13.5	-0.47	176.42597♣

<sup>a</sup>Differences between laser frequency and calculated transition frequency at the magnetic flux density  $B_{obs}$ .<sup>b</sup>Experimental uncertainties (used in the weighted fit).<sup>c</sup>Calculated tuning rates.<sup>d</sup>Calculated transition frequencies for zero field.

\*Lines are unresolved triplets.

the structural properties of the molecule. The new data are of interest not only from a theoretical point of view, but also in relation to studies of interstellar space and of the upper atmosphere.

## II. EXPERIMENTAL DETAILS

The spectra were recorded by far-infrared LMR spectroscopy<sup>17</sup> at the Boulder, Colorado laboratories of NIST. The experimental setup of the LMR apparatus has been described in detail previously.<sup>18</sup> The far-infrared laser is transversely pumped by a CO<sub>2</sub> laser with water-cooled end mirrors and a typical power output of 20 W on a single laser transition. The laser lines used in this work are given in Table I. The frequencies of two of these lines were measured for the first time during this study. One laser line, the 89.13  $\mu\text{m}$  <sup>13</sup>CH<sub>3</sub>OH laser line, was remeasured after the assignment of the H<sub>2</sub>O<sup>+</sup> signals seemed to be impossible. From the H<sub>2</sub>O<sup>+</sup> spectrum, the laser frequency was predicted to be about 0.2 cm<sup>-1</sup> higher than that given in Ref. 19. The remeasurement showed that this prediction was right. The right frequency is given in Table II. A 15-in. electromagnet provides a maximum flux density of 2.0 T. The magnetic flux densities were measured with a Hall probe, which was calibrated with an NMR gaussmeter. The Zeeman modulation frequency was 39 kHz. A liquid helium-cooled germanium-gallium photoconductor was used as the detector.

The H<sub>2</sub>O<sup>+</sup> radicals were produced in the gas phase, using a cw microwave discharge source (50 W). The discharge was run through ultrahigh purity helium (amounts of other gases <1 ppm) at 190 Pa (1.4 torr), with a small amount of water vapor added under flow conditions. The pump system which was used for the cell consists of two parallel rotary pumps providing a maximum pumping speed of about 8 liter/s. The H<sub>2</sub>O<sup>+</sup> signals disappeared rapidly upon the addition of small amounts of H<sub>2</sub>, and were relatively unaffected by the addition of N<sub>2</sub>. This substitution was used to distinguish H<sub>2</sub>O<sup>+</sup> from other species.

The experimental uncertainties of the measurements are caused by the uncertainty of the laser line center ( $\pm 2 \times 10^{-7}$ ), the uncertainty in the magnetic flux density (0.01 mT for  $B < 0.1$  T and  $10^{-4}$  B for  $B > 0.1$  T, and the readout error of the line positions. Thus, the total 1-sigma uncertainty of our data is, at best,  $2 \times 10^{-5}$  cm<sup>-1</sup> (0.6 MHz), depending on the tuning rate of the transition.

## III. RESULTS AND ANALYSIS

Under the experimental conditions described above, 114 Zeeman components of 13 different rotational transitions, with  $N$  up to 7 and  $K_a$  up to 4, have been observed at wavelengths between 50 and 120  $\mu\text{m}$ . Figure 1 shows an energy level diagram of the ground state, in which all measured transitions are marked. The exact line positions of all the Zeeman components are listed in Table II. The maximum signal-to-noise was around 200:1, with a 100 ms time constant.

We observed both singlet and triplet hyperfine patterns according to levels with spin states  $I=0$  ( $K_a + K_c$  odd) and  $I=1$  ( $K_a + K_c$  even). Figure 2 shows a typical spectrum. In

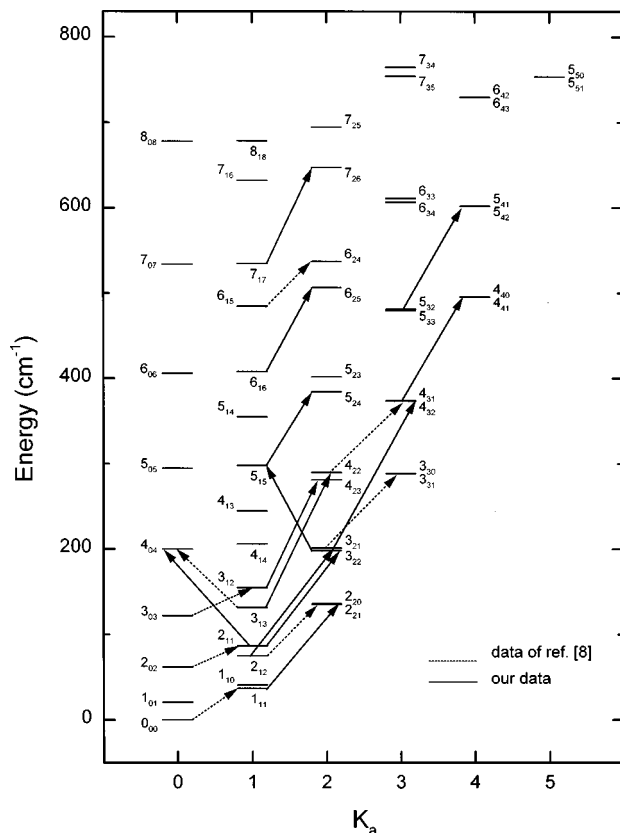


FIG. 1. Energy level diagram of the H<sub>2</sub>O<sup>+</sup> ( $\tilde{X}^2B_1, v=0$ ) state. Transitions observed in this study are marked by solid arrows, and those of Ref. 8 by dotted arrows.

seven cases the triplets could not be resolved. These data are marked in Table II and are provided with low weights corresponding to the large readout errors.

The assignment of transitions, which involved either the 3<sub>22</sub> or the 4<sub>04</sub> states, turned out to be particularly difficult. This is due to the strong mixing between these two states. Thus, the pattern of the corresponding tuning diagrams is complex, and depends very sensitively on the term energies of these states. On the other hand, due to this mixing the 4<sub>04</sub>-2<sub>11</sub> and 5<sub>15</sub>-3<sub>22</sub> ( $\Delta N=2$ ,  $\Delta J=2$ , and 3) transitions gain intensity and can be observed.

Three of the rotational transitions (4<sub>22</sub>-3<sub>13</sub>, 4<sub>40</sub>-4<sub>31</sub>, and 5<sub>42</sub>-5<sub>33</sub>) were observed on two different laser lines, which allowed an accurate determination of the  $g$ -factors. Furthermore, a few transitions with  $\Delta N \neq \Delta J$  could be measured, which enabled an accurate determination of the spin-rotation constants.

The predictions and least-squares fitting of the data were both carried out using a computer program developed by Brown and Sears<sup>20</sup> called ASYTOP. The effective Hamiltonian used by this program was developed by Bowater *et al.*,<sup>21</sup> who explained the derivation of the matrix elements and the assumptions inherent therein. The molecular Hamiltonian is expressed in a Hund's case (b) basis set of  $|NK_aSJM_JIM_I\rangle$  (a nuclear spin-decoupled basis set). For the rotational Hamiltonian, the  $A$  (asymmetric) reduction is used.<sup>22</sup>

The assignment of the LMR spectra was started by using the molecular parameters of Ref. 8 for predictions. Further

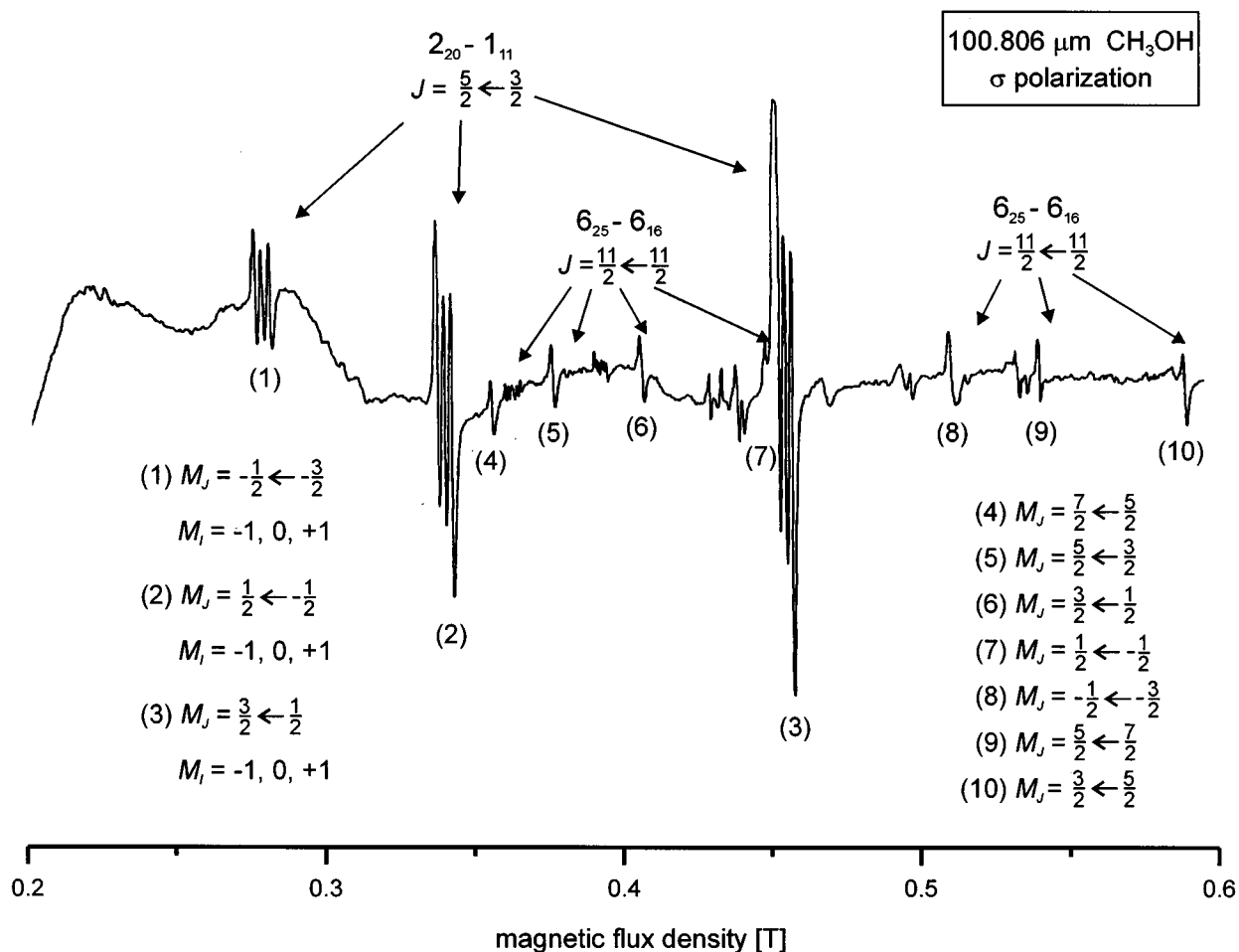


FIG. 2. Typical  $\text{H}_2\text{O}^+$  ( $\tilde{X}^2B_1, \nu=0$ ) LMR spectrum observed at 100.806  $\mu\text{m}$   $\text{CH}_3\text{OH}$  laser line in perpendicular ( $\Delta M_j = \pm 1$ ) polarization. The Zeeman components of the  $2_{20}-1_{11}$  (triplets) and  $6_{25}-6_{16}$  (singlets) transitions are shown.

transitions, especially the strongly perturbed and the transitions with  $N=7$  and  $K_a=4$ , could be assigned only after analysis of the new data.

In the final analysis, previous measurements concerning  $\text{H}_2\text{O}^+$  in the ground state were included in addition to our LMR data. The data which have been used are listed below:

- (1) 96 Zeeman components of 8 rotational transitions in the ground vibrational level of the  $\tilde{X}^2B_1$  state measured by laser magnetic resonance<sup>8</sup> with an experimental uncertainty of 2 MHz
- (2) 28 ground-state combination differences obtained from IR measurements of the  $\nu_3$  band.<sup>10</sup> The uncertainty of the combination differences was  $0.008 \text{ cm}^{-1}$ .
- (3) 251 ground-state combination differences obtained from the  $\tilde{A}^2A_1 - \tilde{X}^2B_1$  electronic emission spectrum.<sup>2</sup> The accuracy of the measurements was  $0.03 \text{ cm}^{-1}$ , giving the combination differences an uncertainty of  $0.04 \text{ cm}^{-1}$ .

In the weighted nonlinear, least-squares fitting procedure, the weights were taken as the inverse squares of the assumed experimental precision (see Table II). As expected from the relative weights of the different data, the fit was

determined principally by the LMR data, although the inclusion of the combination differences obtained from the electronic emission spectrum reduced the correlations between the parameters and did not affect the parameter values. The inclusion of the combination differences from the IR data neither improved nor degraded the parameter values or standard deviations. During the analysis, it turned out that the indirect influence of the levels with  $\Delta N = \pm 1$  and  $\pm 2$  and with  $\Delta K_a = \pm 2, \pm 4, \pm 6$  is considerable. Thus, these levels were all included in the basis set.

Thirty-two molecular parameters were simultaneously determined in the final fit of 375 lines and are listed in Table III. With this set of molecular parameters, all data are reproduced within their experimental precision. The overall standard deviation relative to the experimental uncertainties is 0.88, whereas the deviation between observed and calculated line positions of our LMR data section is 2.2 MHz on average (deviation of LMR data of Ref. 8 is 2.4 MHz on average). Some of the parameters quoted in Table III ( $B, C, \epsilon_{aa}, \epsilon_{bb}, \epsilon_{cc}, a_F, a_I, b_I, g_S^{aa}, g_S^{bb}, g_S^{cc}, g_r^{aa}, g_r^{bb},$  and  $g_r^{cc}$ ) are linear combinations of parameters fitted by the ASYTOP program in order to give a comparison with parameters of pre-

TABLE III. Molecular parameters (in  $\text{cm}^{-1}$ ) for the ground-vibrational level of  $\text{H}_2\text{O}^+$  in the  $\tilde{X}^2B_1$  state (error limits are one standard deviation and refer to the last quoted digits). The A-reduced form of the Hamiltonian was used throughout, apart from Ref. 8, as marked.

Parameter	[12]	[10]	[11]	[2]	[8] (S-reduced)	[8] refitted	This work
A	29.035 9(21)	29.037 0(27)	29.036 6(37)	29.025 6(26)	29.038 365(14)	29.038 99(11)	29.039 508(19)
B	12.422 98(58)	12.423 0(24)	12.417 0(15)	12.422 4(14)	12.416 055(10)	12.421 23(12)	12.420 949(14)
C	8.469 21(58)	8.469 1(16)	8.468 4(13)	8.469 3(14)	8.472 0857(73)	8.468 37(12)	8.468 088(14)
$\Delta_N \times 10^3$	1.015(13)	1.063(14)	0.937(50)	1.00(2)	0.866 89(24)	0.991 7(38)	0.973 96(30)
$\Delta_{NK} \times 10^3$	-5.007(71)	-5.07(6)	-5.63(19)	-4.73(10)	-5.043 8(43)	-5.067(55)	-5.078 8(32)
$\Delta_K \times 10^3$	44.20(63)	43.75(60)	45.72(73)	41.87(18)	44.983 5(73)	45.276(61)	45.716 2(81)
$\delta_N \times 10^3$	0.381 7(24)	0.380 5(41)	0.312(10)	0.370(1)	0.370 83(32)	0.379 3(19)	0.374 77(28)
$\delta_K \times 10^3$	1.795(50)	1.91(10)	1.60(12)	1.97(19)	...	1.815(31)	1.930 8(52)
$H_N \times 10^6$	0.33(14)	1.34(22)	1.89(60)	...	...	...	...
$H_{NK} \times 10^6$	-5.1(11)	-14.3(17)	-9.7(29)	...	...	...	...
$H_{KN} \times 10^6$	...	40(8)	52(21)	...	-83.32(37)	-18.6(49)	-24.21(26)
$H_K \times 10^6$	151(44)	70(31)	203(27)	...	-259.55(70)	205.7(59)	259.35(95)
$H_N^S \times 10^6$	...	...	...	...	...	...	0.126 4(52)
$H_{NK}^S \times 10^6$	...	...	...	...	...	...	-1.440(64)
$H_K^S \times 10^6$	...	...	...	...	...	...	33.70(53)
$L_K \times 10^6$	...	...	...	...	...	...	1.590(27)
$\epsilon_{aa}$	-1.088 2(43)	-1.082 8(51)	-1.104 9(72)	-1.092(18)	-1.089 817(83)	-1.089 199(84)	-1.088 215(63)
$\epsilon_{bb}$	-0.113 0(19)	-0.116 1(22)	-0.123 7(37)	-0.120(8)	-0.114 538(22)	-0.114 552(55)	-0.114 439(41)
$\epsilon_{cc}$	0.003 2(19)	0.002 82(5)	-0.006 1(25)	-0.004(8)	0.001 685(19)	0.001 663(55)	0.001 294(41)
$\Delta_K^S \times 10^3$	6.32(71)	5.63(47)	12.6(8)	5(1)	5.584(12)	5.995(23)	7.456(28)
$(\Delta_{NK}^S + \Delta_{KN}^S) \times 10^3$	-0.72(23)	...	-0.98(4)	...	0.170 8(33)	0.033(13)	-0.543(12)
$\Delta_{NK}^S \times 10^3$	...	...	...	...	...	...	-0.266(22)
$\Delta_N^S \times 10^3$	...	...	...	...	...	...	0.023 4(15)
$\delta_K^S$	...	...	...	...	...	...	...
$\delta_N^S \times 10^3$	...	...	...	...	...	...	0.011 28(81)
$\Phi_K^S \times 10^3$	...	...	...	...	...	...	-0.069 6(13)
$a_F \times 10^3$	...	...	...	...	-2.525 4(70)	-2.518 0(72)	-2.506 2(91)
$a_I \times 10^3$	...	...	...	...	1.308(53)	1.338(28)	1.298(29)
$b_I \times 10^3$	...	...	...	...	-0.577 1(63)	-0.586(24)	-0.600(26)

$^{\#}d_2 = -0.5162(12) \times 10^{-4} \text{cm}^{-1}$  (S-reduction).

vious work. The standard deviations of those parameters have been calculated from the deviation of the quoted parameters according to Gaussian quadrature formula (not taking into account the correlation between parameters).

#### IV. DISCUSSION

The LMR data measured in this work give a significant extension to the measurements of Ref. 8 (see Fig. 1). The analysis of these new rotational transitions in combination with other data published previously leads to an improved set of ground-state molecular parameters (see Tables III and IV).

TABLE IV.  $g$ -factors for the ground-vibrational level of  $\text{H}_2\text{O}^+$  in the  $\tilde{X}^2B_1$  state (error limits are one standard deviation and refer to the last quoted digits).

Parameters	[8]	[8] refitted (A-reduced)	This work	[16] ( <i>ab initio</i> )
$g_S^{aa}$	2.016 46(21)	2.018 33(14)	2.018 86(15)	2.018 052
$g_S^{bb}$	2.006 50(13)	2.006 56(15)	2.006 57(13)	2.006 424
$g_S^{cc}$	1.999 18(21)	2.001 09(15)	2.002 11(13)	2.002 070
$g_r^{aa} \times 10^3$	-6.892(72)	-7.182(39)	-6.742(43)	
$g_r^{bb} \times 10^3$	-0.370(39)	-0.461(32)	-0.586(30)	
$g_r^{cc} \times 10^3$	0.501(32)	0.396(32)	0.421(30)	

Some parameters are determined for the first time and several others are refined. For a comparison, the molecular parameters of earlier studies are also given in Tables III and IV. The constants of Ref. 8 cannot be compared directly with ours because the S-reduced form of the rotational Hamiltonian was used in that work. Thus, we refitted the dataset of Ref. 8 with our program, which uses the A-reduced form. The data fitted slightly better than in Ref. 8, which could be seen from the residuals of each line. But the parameters have larger standard deviations than those for S-reduced Hamiltonian, which is probably due to the higher correlations between the parameters (for example, the spinrotational Hamiltonian has, in A-reduction, only matrix elements for  $\Delta K_a = 0, \pm 2$ ). On the other hand, the Hamiltonian in A-reduced form is easier to bring to diagonal form by computer methods. As seen from the refitted parameters in comparison with ours, we improved the accuracy of the rotational and centrifugal distortion constants by about one order of magnitude. The spin-rotation and the hyperfine splitting parameters, as well as the  $g$ -factors, are of the same accuracy as previous work.

As mentioned before, a number of *ab initio* calculations have been carried out on  $\text{H}_2\text{O}^+$ ; some of them investigated the hyperfine coupling constants of the ground state. A good agreement with the experimental value  $a_F = -75.13(27)$

TABLE V. Rotational term values (in  $\text{cm}^{-1}$ ) for the  $\tilde{X}^2B_1$  ground state [ $T(0_{00})=0$ ].

N	$K_a$	$K_c$	[2]	$F_1$		[2]	$F_2$	
				this work <sup>a</sup>	difference		this work <sup>a</sup>	difference
1	0	1	20.857	20.85524	0.002	20.950	20.93747	0.013
1	1	1	37.188	37.19741	-0.009	38.010	38.01100	-0.001
1	1	0	41.100	41.11005	-0.010	42.010	42.01115	-0.001
2	0	2	61.955	61.95144	0.004	62.109	62.09015	0.019
2	1	2	75.094	75.10327	-0.009	75.612	75.60769	0.004
2	1	1	86.845	86.85337	-0.008	87.508	87.50238	0.006
2	2	1	135.672	135.67974	-0.008	137.516	137.50442	0.012
2	2	0	136.293	136.30047	-0.007	138.139	138.12768	0.011
3	0	3	122.117	122.11128	0.006	122.329	122.30162	0.027
3	1	3	131.478	131.48612	-0.008	131.899	131.88851	0.010
3	1	2	154.892	154.89891	-0.007	155.516	155.50345	0.013
3	2	2	198.465	198.47342	-0.008	199.900	199.88923	0.011
3	2	1	201.483	201.49353	-0.011	202.900	202.88966	0.010
3	3	1	288.757	288.71477	0.042	291.565	291.48641	0.079
3	3	0	288.820	288.77799	0.042	291.628	291.54944	0.079
4	0	4	200.025	200.01810	0.007	200.313	200.27990	0.033
4	1	4	205.979	205.98667	-0.008	206.362	206.34565	0.016
4	1	3	244.589	244.59297	-0.004	245.235	245.21233	0.023
4	2	3	281.534	281.54461	-0.011	282.742	282.73042	0.012
4	2	2	289.900	289.91232	-0.012	291.119	291.10722	0.012
4	3	2	373.658	373.62281	0.035	375.952	375.88588	0.066
4	3	1	374.086	374.05256	0.033	376.379	376.31520	0.064
4	4	1	495.619	495.63116	-0.012	499.316	499.28331	0.033
4	4	0	495.625	495.63661	-0.012	499.321	499.28873	0.032
5	0	5	294.755	294.75126	0.004	295.064	295.02871	0.035
5	1	5	298.215	298.22460	-0.010	298.584	298.56418	0.020
5	1	4	354.940	354.94082	-0.001	355.631	355.59952	0.031
5	2	4	384.372	384.38380	-0.012	385.471	385.45552	0.015
5	2	3	401.892	401.90610	-0.014	403.024	403.00826	0.016
5	3	3	479.658	479.62753	0.030	481.661	481.60218	0.059
5	3	2	481.310	481.28466	0.025	483.298	483.24382	0.054
5	4	2	601.896	601.91096	-0.015	605.041	605.02309	0.018
5	4	1	601.943	601.95841	-0.015	605.088	605.07030	0.018
5	5	1	753.374	754.10064	-0.727	757.847	758.56849	-0.721
5	5	0	753.375	754.10108	-0.726	757.847	758.56893	-0.722
6	0	6	405.959	405.96298	-0.004	406.295	406.26257	0.032
6	1	6	407.850	407.86446	-0.014	408.216	408.19591	0.020
6	1	5	484.628	484.62744	0.001	485.391	485.35102	0.040
6	2	5	506.463	506.47296	-0.010	507.503	507.48216	0.021
6	2	4	537.054	537.06921	-0.015	538.163	538.14097	0.022
6	3	4	606.602	606.57058	0.031	608.411	608.35111	0.060
6	3	3	611.193	611.17539	0.018	612.988	612.94083	0.047
6	4	3	729.401	729.40645	-0.005	732.181	732.16135	0.020
6	4	2	729.625	729.63319	-0.008	732.405	732.38738	0.018
6	5	2	881.026	881.71322	-0.687	884.938	885.63219	-0.694
6	5	1	881.031	881.71785	-0.687	884.943	885.63679	-0.694
6	6	1	1058.043	1061.18641	-3.143	1063.144	1066.44230	-3.298
6	6	0	1058.043	1061.18645	-3.143	1063.144	1066.44234	-3.298
7	0	7	533.622	533.63891	-0.017	533.977	533.95252	0.024
7	1	7	534.618	534.64207	-0.024	534.986	534.97079	0.015
7	1	6	632.208	632.20692	0.001	633.028	632.98227	0.046
7	2	6	647.235	647.24129	-0.006	648.246	648.21722	0.029
7	2	5	694.445	694.46266	-0.018	695.570	695.54222	0.028
7	3	5	754.111	754.06797	0.043	755.800	755.72758	0.072
7	3	4	764.440	764.43060	0.009	766.114	766.06994	0.044
7	4	4	878.125	878.10375	0.021	880.642	880.60015	0.042
7	4	3	878.891	878.87692	0.014	881.417	881.38257	0.034
7	5	3	1029.806	1030.41256	-0.607	1033.319	1033.94360	-0.625
7	5	2	1029.832	1030.43888	-0.607	1033.345	1033.96977	-0.625
7	6	2	1207.209	1210.18753	-2.979	1211.762	1214.89537	-3.133
7	6	1	1207.210	1210.18796	-2.978	1211.762	1214.89579	-3.134
7	7	1	1404.729	1413.24240	-8.513	1410.279	1419.33848	-9.059
7	7	0	1404.729	1413.24241	-8.513	1410.279	1419.33848	-9.059
8	0	8	677.812	677.84256	-0.031	678.180	678.16476	0.015
8	1	8	678.325	678.36124	-0.036	678.699	678.69030	0.009
8	1	7	796.481	796.47789	0.003	797.359	797.30741	0.052

TABLE V. (Continued.)

N	K <sub>a</sub>	K <sub>c</sub>	[2]	F <sub>1</sub>		[2]	F <sub>2</sub>	
				this work <sup>a</sup>	difference		this work <sup>a</sup>	difference
8	2	7	806.133	806.13224	0.001	807.133	807.09234	0.041
8	2	6	872.817	872.83927	-0.022	873.972	873.93947	0.033
8	3	6	921.690	921.62226	0.068	923.306	923.20489	0.101
8	3	5	941.393	941.39527	-0.002	942.998	942.95742	0.041
8	4	5	1047.905	1047.82940	0.076	1050.263	1050.16996	0.093
8	4	4	1050.072	1050.02039	0.052	1052.417	1052.34681	0.070
8	5	4	1199.684	1200.15716	-0.473	1202.906	1203.40505	-0.499
8	5	3	1199.788	1200.26410	-0.476	1203.010	1203.51155	-0.502
8	6	3	1377.378	1380.08500	-2.707	1381.521	1384.38775	-2.867
8	6	2	1377.380	1380.08780	-2.708	1381.524	1384.39053	-2.867
8	7	2	1575.591	1583.66732	-8.076	1580.621	1589.21377	-8.593
8	7	1	1575.591	1583.66736	-8.076	1580.621	1589.21381	-8.593
8	8	1	1787.638	1805.01081	-17.373	1793.423	1812.12896	-18.706
8	8	0	1787.638	1805.01081	-17.373	1793.423	1812.12896	-18.706

<sup>a</sup>The estimated uncertainties of the term values are about 0.00004 cm<sup>-1</sup> for levels up to N=7 and K<sub>a</sub>=4. All other term energies are extrapolated.

MHz is achieved in Ref. 14. This group calculated the hyperfine coupling constant *a<sub>F</sub>* to be -81.0 MHz by the multireference configuration method, which is within 10% of the experimental value. Recently, a multireference configuration interaction calculation of electronic *g*-tensors was carried out.<sup>16</sup> This group obtained values for the anisotropic *g*-tensor components Δ*g<sub>l</sub><sup>aa</sup>*, Δ*g<sub>l</sub><sup>bb</sup>*, and Δ*g<sub>l</sub><sup>cc</sup>* (differences between the actual *g*-tensor components along molecule-fixed axes and the free electron *g*-factor *g<sub>S</sub>*=2.002 319) of 0.015 733, 0.004 105, and -0.000 249, respectively, which are in excellent agreement with the experimental values of 0.016 54(15), 0.004 25(13), and -0.000 21(13), respectively (see also Table IV).

From our set of molecular parameters, we recalculated the term values of the ground-state rotational level up to N = 8 and compared them to those of Ref. 2 (see Table V).

TABLE VI. Zero-field predictions of the 1<sub>11</sub>-0<sub>00</sub> transition frequencies (in cm<sup>-1</sup>) including hyperfine splitting.

J'	J''	F'	F''	Transition frequency <sup>a</sup>	Relative intensity calculated <sup>b</sup>
3/2	1/2	5/2	1/2	37.19544	(not allowed)
3/2	1/2	3/2	1/2	37.19741	20
3/2	1/2	1/2	1/2	37.19860	16
3/2	1/2	5/2	3/2	37.19920	54
3/2	1/2	3/2	3/2	37.20117	16
3/2	1/2	1/2	3/2	37.20236	2
1/2	1/2	1/2	1/2	38.01100	2
1/2	1/2	3/2	1/2	38.01165	16
1/2	1/2	1/2	3/2	38.01475	16
1/2	1/2	3/2	3/2	38.01541	20

<sup>a</sup>Absolute uncertainties of the transition wavenumbers are about 0.00006 cm<sup>-1</sup>. Relative uncertainties are smaller than this.

<sup>b</sup>Calculated according to the relation:

$$\text{Intensity} \propto (2F'+1)(2F+1) \begin{Bmatrix} I & J' & F' \\ 1 & F & J \end{Bmatrix}^2 (2J'+1)(2J+1) \\ \times \begin{Bmatrix} S & N' & J' \\ 1 & J & N \end{Bmatrix}^2 (2N'+1)(2N+1) \begin{Bmatrix} N' & 1 & N \\ -K' & 1 & K \end{Bmatrix}^2$$

Large deviations exist for levels with K<sub>a</sub>=3 and with K<sub>a</sub> > 4 (a difference larger than the absolute accuracy of 0.05 cm<sup>-1</sup> mentioned in Ref. 2). The large differences for K<sub>a</sub> > 4 levels (for K<sub>a</sub>=5 about 0.7 cm<sup>-1</sup>, for K<sub>a</sub>=6 about 3 cm<sup>-1</sup>, for K<sub>a</sub>=7 about 9 cm<sup>-1</sup>, and for K<sub>a</sub>=8 about 17 cm<sup>-1</sup>) are because those term values are only extrapolated from measurements involving levels with K<sub>a</sub> ≤ 4, but the differences of the K<sub>a</sub>=3 levels (up to 0.08 cm<sup>-1</sup>) cannot be explained.

Table VI gives zero-field predictions of the 1<sub>11</sub>-0<sub>00</sub> transition including hyperfine splitting (see Fig. 3). Calculations of relative intensities are also given. Measurements using a TUFIR spectrometer would give more accurate line frequencies, which in turn would help astrophysicists identify H<sub>2</sub>O<sup>+</sup> from far-infrared lines in comets or interstellar clouds.

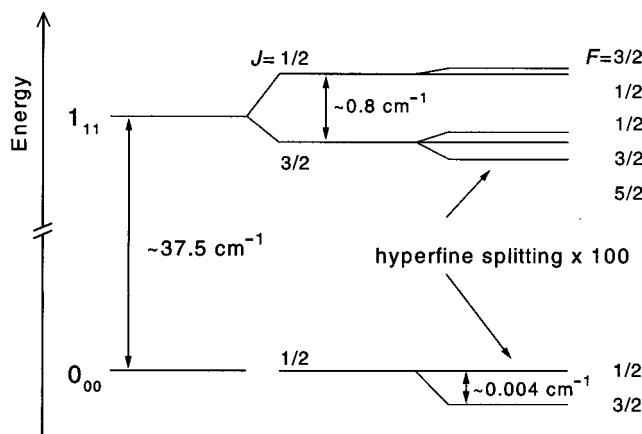


FIG. 3. Energy level diagram (including hyperfine splitting) of the 1<sub>11</sub>-0<sub>00</sub> transition of H<sub>2</sub>O<sup>+</sup> in the (0,0,0) level of the  $\tilde{X}^2B_1$  state.

**ACKNOWLEDGMENTS**

We thank Lew Mullen for valuable technical assistance during the course of the experimental work. We acknowledge Kristine Hensel for helping us during the analysis of the data. One of us (P.M.) is grateful to NIST for financial support and for the warm hospitality during her stay. Work supported by NASA grant No. W-19, 187.

- <sup>1</sup>H. Lew and I. Heiber, *J. Chem. Phys.* **58**, 1246 (1973).
- <sup>2</sup>H. Lew, *Can. J. Phys.* **54**, 2028 (1976).
- <sup>3</sup>G. Herzberg and H. Lew, *Astron. Astrophys.* **31**, 123 (1974).
- <sup>4</sup>P. A. Wehinger, S. Wyckoff, G. H. Herbig, G. Herzberg, and H. Lew, *Astrophys. J.* **190**, L43 (1974).
- <sup>5</sup>Y. P. Viala, *Astron. Astrophys., Suppl. Ser.* **64**, 391 (1986).
- <sup>6</sup>G. Herzberg, *Ann. Geophys. (C.N.R.S.)* **36**, 605 (1980).
- <sup>7</sup>B. Das and J. W. Farley, *J. Chem. Phys.* **95**, 8809 (1991).
- <sup>8</sup>S. E. Strahan, R. P. Mueller, and R. J. Saykally, *J. Chem. Phys.* **85**, 1252 (1986).
- <sup>9</sup>D.-J. Liu, W.-C. Ho, and T. Oka, *J. Chem. Phys.* **87**, 2442 (1987).
- <sup>10</sup>B. M. Dinelli, M. W. Crofton, and T. Oka, *J. Mol. Spectrosc.* **127**, 1 (1988).
- <sup>11</sup>P. R. Brown, P. B. Davies, and R. J. Stickland, *J. Chem. Phys.* **91**, 3384 (1989).
- <sup>12</sup>T. R. Huet, C. J. Pursell, W. C. Ho, B. M. Dinelli, and T. Oka, *J. Chem. Phys.* **97**, 5977 (1992).
- <sup>13</sup>T. R. Huet, I. Hadj Bachir, and J.-L. Destombes, *J. Chem. Phys.* **107**, 5645 (1997).
- <sup>14</sup>M. Staikova, B. Engels, M. Peric, and S. D. Peyerimhoff, *Mol. Phys.* **80**, 1485 (1993).
- <sup>15</sup>H. Nakatsuji, M. Ehara, and T. Momose, *J. Chem. Phys.* **100**, 5821 (1994).
- <sup>16</sup>G. H. Lushington and F. Grein, *J. Chem. Phys.* **106**, 3292 (1997).
- <sup>17</sup>K. M. Evenson, R. J. Saykally, D. A. Jennings, R. F. Curl, and J. M. Brown, in *Chemical and Biochemical Application of Lasers*, edited by C. B. Moore (Academic, New York, 1980), Vol. V.
- <sup>18</sup>S. H. Ashworth, K. M. Evenson, and J. M. Brown, *J. Mol. Spectrosc.* **172**, 282 (1995).
- <sup>19</sup>L.-H. Xu, R. M. Lees, E. C. C. Vasconcellos, L. R. Zink, K. M. Evenson, S. C. Zerbetto, and A. Predoi, *J. Opt. Soc. Am. B* **12**, 2352 (1995).
- <sup>20</sup>J. M. Brown and T. J. Sears, *J. Mol. Spectrosc.* **75**, 111 (1979).
- <sup>21</sup>I. C. Bowater, J. M. Brown, and A. Carrington, *Proc. R. Soc. London, Ser. A* **333**, 265 (1973).
- <sup>22</sup>J. K. G. Watson, in *Vibrational Spectra and Structure*, edited by J. R. Durig (Elsevier, Amsterdam, 1997), Vol. 6, Chap. 1.
- <sup>23</sup>J. O. Henningsen and J. C. Petersen, *Infrared Phys.* **18**, 475 (1978).
- <sup>24</sup>N. G. Douglas, *Millimeter and Submillimeter Wavelength Lasers* (Springer, Berlin, 1989).